Fluorescent Probes

DOI: 10.1002/anie.200701720

A Two-Photon Fluorescent Probe for Calcium Waves in Living Tissue**

*Hwan Myung Kim, Bo Ra Kim, Jin Hee Hong, Jin-Sung Park, Kyoung J. Lee, and Bong Rae Cho**

Calcium is a versatile intracellular signal messenger that controls numerous cellular functions.[1] The Ca^{2+} signaling system operates in many different ways to regulate various cellular processes that function over a wide dynamic range. Calcium triggers exocytosis within microseconds and drives the gene transcription and proliferation in minutes to hours. The concentration of this ion varies from 100 nM at rest to 1 μM upon activation.[1] To understand these functions, fluorescence imaging—with fluorescent probes such as Oregon Green 488 BAPTA-1 (OG1) and fura-2—has often been applied.[2,3] However, the use of these probes with one-photon microscopy requires excitation with short-wavelength light (that is, ca. 350–500 nm). This requirement limits their applications in tissue imaging due to the shallow penetration depth (less than 100 μm) as well as the photobleaching, photodamage, and cellular autofluorescence.[3–5] Two-photon microscopy (TPM) overcomes these problems. The technique, which employs two lower-energy, near-infrared photons for excitation, has the advantages of an increased penetration depth (greater than 500 μm), a localized excitation, and a prolonged observation time. Thus, TPM allows imaging deep inside tissues for a long period of time without interference from artifacts of surface preparation, which can extend more than 70 μm into the tissue slice.[6] However, most of the fluorescent probes presently used for TPM have small two-photon action cross sections ($\Phi\delta$), thus demanding impractically high probe concentrations and/or a high laser power.[7,8] Furthermore, the fluorescence signals from membrane-bound probes can cause significant errors, such as mistargeting,[2,4,9] because the fluorescence quantum yield is higher in the membrane than in the cytosol. Therefore, there is a need to develop efficient two-photon (TP) probes that allow visualization of the calcium activity deep inside living tissues without photobleaching or mistargeting problems.

To design a TP probe for calcium activity, we considered the following requirements: i) A significant TP cross section to obtain bright TPM images at low probe concentrations; ii) a high selectivity for Ca^{2+} ions; iii) large spectral shifts in different environments for discrimination between the cytosolic and membrane-bound probes; and iv) high photostability. Here, we extend our earlier work with specific ion probes[10] and present a novel TP probe (namely, ACa1) for intracellular free Ca^{2+} ions; this probe is derived from 2-acetyl-6-(dimethylamino)naphthalene as the TP chromophore[10b] and *O*,*O*′-bis(2-aminophenyl)ethyleneglycol-*N*,*N*,*N*′,*N*′-tetraacetic acid (abbreviated BAPTA) as the Ca^{2+}-ion chelator.[11] ACa1 shows a significant TP cross section and large spectral shifts with the solvent polarity (Scheme 1), thus allowing the detection of the two-photon

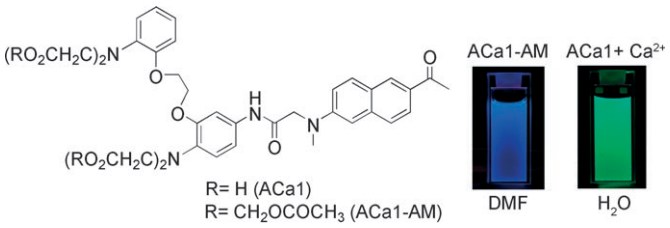

Scheme 1. The structures of ACa1 and ACa1-AM.

excited fluorescence (TPEF) of the ACa1–Ca^{2+} complex separately from that of membrane-bound probes. Herein, we report that ACa1 is capable of imaging calcium waves in living cells and living tissues (at greater than 100 μm depth) for a long period of time without any mistargeting or photobleaching problems.

ACa1 was prepared (with a 53% yield) from 6-acyl-2-[*N*-methyl-*N*-(carboxymethyl)amino]naphthalene and 5-amino-BAPTA-tetramethyl ester (see the Supporting Information). To enhance the cell permeability, the carboxylic-acid moieties were converted into acetoxymethyl esters (ACa1-AM).[11b]

The absorption and emission spectra of ACa1-AM showed gradual red shifts with the solvent polarity in the order: 1,4-dioxane < dimethylformamide (DMF) < ethanol (EtOH) < H_2O (see Figure S1 and Table S1 in the Supporting Information). The effect was greater for the emission (82 nm) than for the absorption spectrum (17 nm), thus indicating the utility of this compound as a polarity probe. In addition, the value of λ_{max}^{fl} for ACa1-AM in DMF was similar to that of the membrane-bound probes (see Figure 2b and Figure S1b of

[*] H. M. Kim, B. R. Kim, Prof. Dr. B. R. Cho
Department of Chemistry and Center
for Electro- and Photoresponsive Molecules
Korea University, 1-Anamdong
Seoul, 136-701 (Korea)
Fax: (+82) 2-3290-3544
E-mail: chobr@korea.ac.kr
Dr. J. H. Hong, Dr. J.-S. Park, Prof. Dr. K. J. Lee
National Creative Research Initiative Center
for Neurodynamics and Department of Physics
Korea University, 1-Anamdong
Seoul, 136-701 (Korea)

[**] This work was supported by KRF-2004-201-C00067. J.H.H. and K.J.L. were supported by Creative Research Initiatives of the Korean Ministry of Science and Technology.

Supporting information for this article is available on the WWW under http://www.angewandte.org or from the author.

the Supporting Information), which suggests that this system can be used as a model for membrane-bound probes (see below).

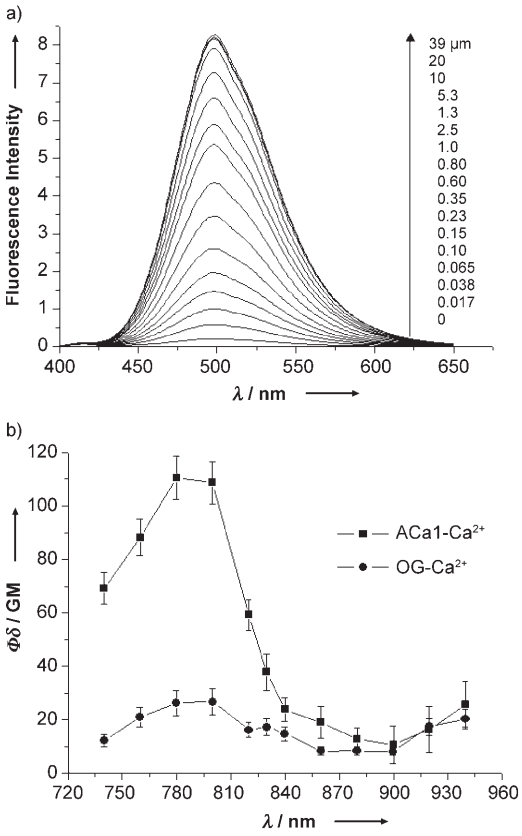

Figure 1. a) One-photon fluorescence spectra of 1 μM ACa1 (30 mM MOPS, 100 mM KCl, 10 mM EGTA, pH 7.2) in the presence of free Ca^{2+} ions (0–39 μM). b) Two-photon action spectra of ACa1 (■) and OG1 (●) in the presence of 39 μM free Ca^{2+} ions.

When Ca^{2+} ions were added to ACa1 in a 3-(*N*-morpholino)propanesulfonic acid (MOPS) buffer solution (30 mM, pH 7.2), the fluorescence intensity increased dramatically as a function of the metal-ion concentration (without affecting the absorption spectra, see Figure 1a and Figure S2a of the Supporting Information). This behavior is probably caused by a blocking of the photoinduced-electron-transfer (PET) process as a result of the complexation of the metal ion. A nearly identical result was observed in the two-photon process (Figure S2b, Supporting Information). The fluorescence-enhancement factor $[(F-F_{min})/F_{min}]$ of ACa1 was 40 in the presence of 39 μM Ca^{2+}, that is, nearly three times larger than the value (of 14) previously reported for OG1.[2] Moreover, linear Hill plots determined for the Ca^{2+} and Mg^{2+} binding (with slopes of 1.0) indicated a 1:1 complexation between the probe and the cations (see Figure S2c in the Supporting Information).[12]

The dissociation constants (K_d^{OP}) were calculated from the fluorescence titration curves (see Figure S2d in the Supporting Information), as reported in reference [13]. The K_d^{OP} values of ACa1 for Ca^{2+} and Mg^{2+} were (0.27 ± 0.01) μM and (6.8 ± 0.7) mM, respectively. A similar value was determined in the two-photon process $[K_d^{TP}\ (Ca^{2+}) = (0.25 \pm 0.03)$ μM] (see Table S2, Supporting Information). ACa1 showed a modest response toward Zn^{2+} and Mn^{2+}, a much weaker response toward Mg^{2+}, Fe^{2+}, and Co^{2+}, and no response toward Cu^{2+} (Figure S4a, Supporting Information). Since the intracellular concentration of free Mn^{2+} ions is negligible, this probe can selectively detect the intracellular concentration of Ca^{2+} ions (namely, $[Ca^{2+}]_i$) in the regions where the concentration of chelatable Zn^{2+} (namely, $[Zn^{2+}]_i$) is much lower than K_d^{TP} (Ca^{2+}). Furthermore, ACa1 is pH-insensitive in the biologically relevant pH range (see Figure S4b of the Supporting Information).

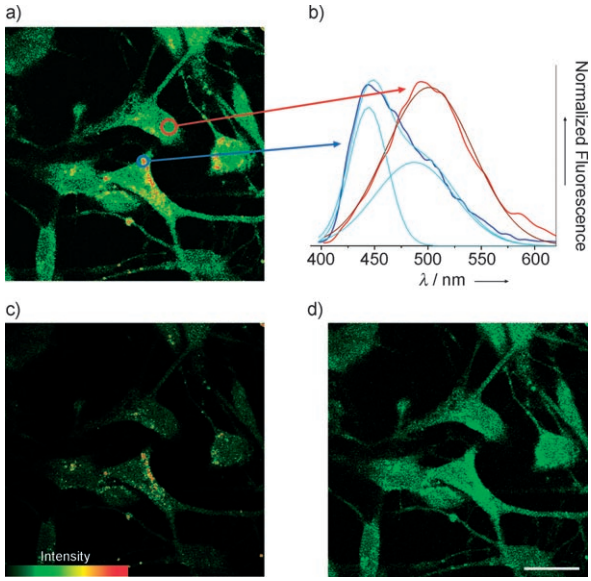

Figure 2. Pseudocolored TPM images of ACa1-AM-labeled (2 μM) astrocytes collected at 360–620 nm (a), 360–460 nm (c), and 500–620 nm (d). b) Two-photon excited fluorescence spectra of the hydrophobic (dark blue) and hydrophilic (red) domains of ACa1-AM-labeled astrocytes. The light blue and brown curves represent the dissected Gaussian functions for the dark blue and red bands, respectively. The excitation wavelength was 780 nm. The cells shown are representative images from replicate experiments. Scale bar: 30 μm.

The TP action spectra of the Ca^{2+} complexes with ACa1 and OG1 in buffer solutions indicated that $\Phi\delta = 110$ GM for the ACa1–Ca^{2+} complex at 780 nm, a value that is fivefold that of the OG1–Ca^{2+} complex (see Figure 1b and Table S2, Supporting Information). Thus, the TPM images of samples stained with ACa1 would be much brighter than those stained with the commercial probe. In addition, the two-photon fluorescence-enhancement factor (TPFEF), estimated from the TP titration curve, was 44 (Table S2, Supporting Information), a value that allowed the detection of Ca^{2+} ions by using TPM.

The pseudocolored TPM images of cultured astrocytes labeled with 2 μM ACa1-AM showed intense spots and homogeneous domains (Figure 2a). We attributed these images to the TPEF emitted from the intracellular ACa1–Ca^{2+} complex and the membrane-bound probes, because the fluorescence quantum yields of the ACa1–Ca^{2+} complex in the MOPS buffer (with a value of 0.49) and of ACa1-AM in

DMF (with a value of 0.27) are much higher than those of ACa1 (namely, 0.012) and ACa1-AM (namely, 0.060) in the MOPS buffer (see Table S2, Supporting Information). Furthermore, the system composed by ACa1-AM in DMF has been assumed to be a good model for the membrane-bound probes because of the similar λ_{max}^{fl} values (see above).

The TPEF spectra of the intense spots and homogeneous domains showed emission maxima at 445 (Figure 2b, dark blue curve) and 494 nm (Figure 2b, red curve), respectively. Moreover, the blue emission band was asymmetrical and could be fitted to two Gaussian functions with emission maxima at 445 and 488 nm (Figure 2b, light blue curves), whereas the red emission band could be fitted to a single Gaussian function with maximum at 500 nm (Figure 2b, brown curve). The shorter-wavelength band of the dissected spectrum was significantly blue-shifted relative to that of the emission spectra recorded in the MOPS buffer (Figure 1a), while the longer-wavelength band remained unchanged. The spectral shift suggests that the probes may be located in two regions of different polarity. To assess the polarity of the environment, lifetime images of ACa1-AM-labeled astrocytes were obtained. The intense spots exhibited an excited-state lifetime of 1.8 ns (which is more than two times longer than the upper limit of the lifetime-distribution curve centered at about 0.8 ns, see Figure S5 of the Supporting Information). This result may reflect the existence of two distinct environments populated by this probe: a hydrophilic one, which is likely to be cytosolic and emits red light with a shorter lifetime, and a hydrophobic one, which is likely to be membrane-associated and exhibits a longer-lived blue emission.

The intracellular Ca^{2+} ions could be detected with minimum errors attributed to the membrane-bound probes. The spectrum of the shorter-wavelength band in the dissected Gaussian function (Figure 2b, light blue curve) decreased to the baseline at about 500 nm, thus indicating that the interference caused by the TPEF emitted from the membrane-bound probes is negligible at $\lambda > 500$ nm. Similarly, if one considers the system composed by ACa1-AM in DMF as a model for membrane-bound probes (see above), the fluorescence at $\lambda > 500$ nm accounts for only 5% of the total emission band (Figure S1b, Supporting Information). Consistently, the TPM image collected at 500–620 nm is homogeneous, and hence has no intense spots (see Figure 2d), whereas the one collected at 360–460 nm clearly shows them (Figure 2c). Therefore, one can selectively detect the intracellular Ca^{2+} ions by using the detection window at 500–620 nm.

To demonstrate the utility of this probe, we monitored the $[Ca^{2+}]_i$ activity in cells and living tissue. The TPM images of cultured astrocytes labeled with 2 μM ACa1-AM revealed a spontaneous Ca^{2+}-signal propagation from the astrocytic process (1) to the soma (2) and to the terminal (3), with a speed of $(7.5 \pm 2.2)\ \mu m\,s^{-1}$ ($n = 5$ astrocytes, Figure 3a,c and Movie S1, Supporting Information). The spontaneous increase in $[Ca^{2+}]_i$ also propagated between astrocytes, as indicated by the delayed activity in the neighboring astrocyte (Figure 3b,d). The speed of propagation of spontaneously occurring waves was $(1.8 \pm 1.1)\ \mu m\,s^{-1}$ ($n = 7$ astrocytes), a result consistent with the reported data.[14] Thus, ACa1 is clearly capable of visualizing the intra- and intercellular calcium waves in cultured astrocytes by using TPM.

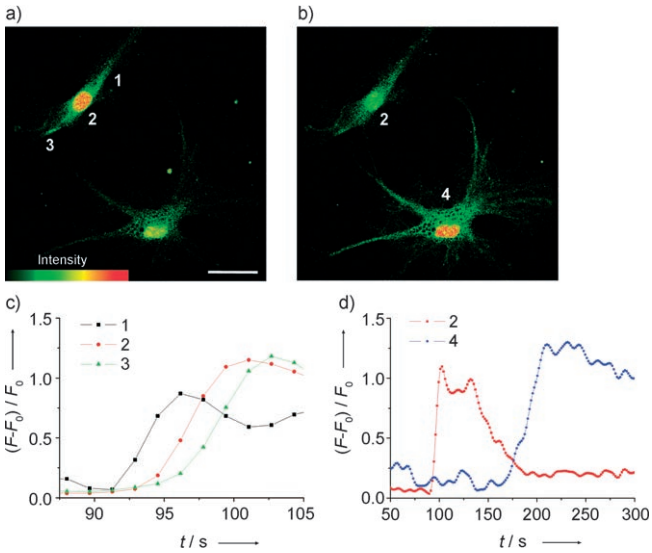

Figure 3. Pseudocolored TPM images of 2 μM ACa1-AM-labeled astrocytes taken after a) 110 and b) 220 s. c,d) Time courses of the calcium waves in different locations showing the spontaneous intracellular [curves 1–3 in (c)] and intercellular [curves 2 and 4 in (d)] Ca^{2+} propagation. The images were collected at 500–620 nm (with intervals of 1.6 s) using an excitation wavelength of 780 nm. Scale bar: 30 μm.

We further investigated the utility of this probe in tissue imaging. TPM images were obtained for individual astrocytes in acute hypothalamic slices from a one-day-old rat (Figure 4). The slices were incubated with 10 μM ACa1-AM

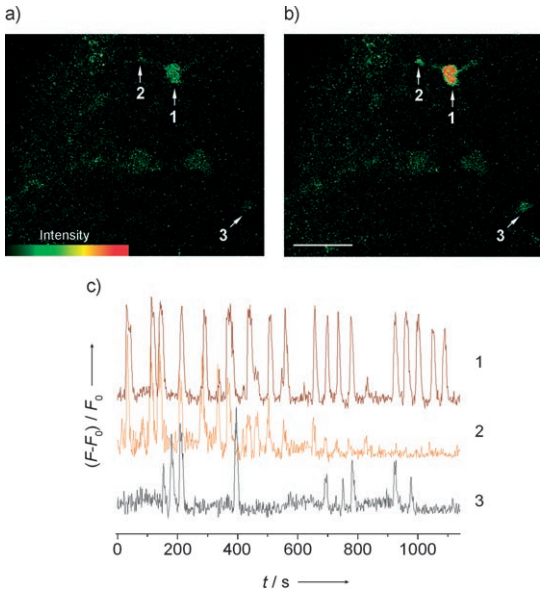

Figure 4. a,b) Pseudocolored TPM images of an acute rat hypothalamic slice stained with 10 μM ACa1-AM taken after 195 (a) and 214 s (b). Magnification at 100× shows the hypothalamic area at a depth of about 170 μm. c) Spontaneous Ca^{2+} transients recorded in the soma (1), the astrocyte process (2), and a neighboring cell (3). The TPEF images were collected at 500–620 nm upon excitation at 780 nm with fs pulses. Scale bar: 30 μm.

for 30 min at 37 °C. The spontaneous Ca^{2+} waves in the soma (Figure 4, trace 1) could be clearly visualized, with a frequency of about 16 mHz ($n = 4$ slices), for more than 1100 s and without appreciable decay (see Movie S2, Supporting Information). Furthermore, the spikes appeared somewhat earlier in the astrocyte process (Figure 4, trace 2) than in the soma (Figure 4, trace 1), which confirms the previous finding[14] that the signals propagate progressively from the process to the soma. Similar results were reported for tetrodotoxin (TTX) treated thalamus slices stained with fura-2,[14] except that the image revealed damaged cells on the tissue surface and was not as clear as the TPM image presented here. Also, the fluorescence intensity decayed appreciably after 500 s.[14] The improved TPM image of ACa1-labeled tissue, obtained at a depth of about 170 μm for a prolonged observation time, underlines the high photostability and low phototoxicity of this probe, in addition to the capability of deep tissue imaging. Similar calcium spikes were also observed in a different cell (Figure 4, trace 3).

We also visualized the $[Ca^{2+}]_i$ distribution in the CA1 region by means of TPM (using ACa1). Although the value of $[Zn^{2+}]_i$ is much lower in the CA1 than in the CA3 region,[15] the exact concentration range is not known. If $[Zn^{2+}]_i \ll K_d^{TP}$-(Ca^{2+}), this probe can selectively detect $[Ca^{2+}]_i$ in this region. To investigate this possibility, we obtained TPM images of the pyramidal neuron layer of the CA1 region. The bright-field image of a part of a rat-hippocampal slice shows the CA1 and CA3 regions as well as the dentate gyrus (see Figure S6a in the Supporting Information). The TPM image revealed the same regions at a depth of about 150 μm (Figure S6b, Supporting Information). Moreover, the TPM images of the pyramidal neuron layer of the CA1 region [taken with and without previous treatment with a 20 μM Zn^{2+} solution, chelator: *N*,*N*,*N*′,*N*′-tetrakis(2-pyridylmethyl)ethylenediamine (TPEN)] show the same intensity (see Figures S6c and S6d, Supporting Information). It is well known that TPEN is a membrane-permeable Zn^{2+} chelator that can effectively remove Zn^{2+} ions by chelation without causing any toxic effect.[16] These results indicate that ACa1 can selectively detect $[Ca^{2+}]_i$ with almost no interference from the Zn^{2+} ions. Moreover, the $[Ca^{2+}]_i$ distribution can be clearly visualized with this probe in the CA1 region—at a depth of 80–200 μm—by using TPM (Figure S7, Supporting Information).

In conclusion, we developed a TP probe (namely, ACa1) that shows a 44-fold TPEF enhancement in the response to Ca^{2+} species, has a dissociation constant (K_d^{TP}) of (0.25 ± 0.03) μM, and emits a fivefold stronger TPEF signal than that of OG1 upon complexation with Ca^{2+} ions. Unlike the previously available probes, this novel probe can selectively detect dynamic levels of intracellular free Ca^{2+} ions in living cells and living tissues without interference from other metal ions and without contributions from the membrane-bound probes. Moreover, by using TPM, this probe is capable of monitoring the calcium waves at a depth of about 150 μm in living tissues for more than 1100 s and with no photobleaching artifacts.

Received: April 18, 2007
Published online: August 6, 2007

Keywords: calcium · fluorescence · microscopy · two-photon probes

[1] a) M. J. Berridge, M. D. Bootman, H. L. Roderick, *Nat. Rev. Mol. Cell Biol.* **2003**, *4*, 517–529; b) S. Orrenius, B. Zhivotovsky, P. Nicotera, *Nat. Rev. Mol. Cell Biol.* **2003**, *4*, 552–565; c) R. Rizzuto, T. Pozzan, *Physiol. Rev.* **2006**, *86*, 369–408.
[2] *A Guide to Fluorescent Probes and Labeling Technologies*, *10th ed.* (Ed.: R. P. Haugland), Molecular Probes, Eugene, **2005**.
[3] R. Rudolf, M. Mongillo, R. Rizzuto, T. Pozzan, *Nat. Rev. Mol. Cell Biol.* **2003**, *4*, 579–586.
[4] D. Thomas, S. C. Tovey, T. J. Collins, M. D. Bootman, M. J. Berridge, P. Lipp, *Cell Calcium* **2000**, *28*, 213–223.
[5] a) D. A. Williams, F. S. Fay, *Am. J. Physiol.* **1986**, *250*, C779–C791; b) E. Grapengiesser, *Cell Struct. Funct.* **1993**, *18*, 3–17.
[6] a) R. M. Williams, W. R. Zipfel, W. W. Webb, *Curr. Opin. Chem. Biol.* **2001**, *5*, 603–608; b) M. D. Cahalan, I. Parker, S. H. Wei, M. J. Miller, *Nat. Rev. Immunol.* **2002**, *2*, 872–880; c) W. R. Zipfel, R. M. Williams, W. W. Webb, *Nat. Biotechnol.* **2003**, *21*, 1369–1377; d) F. Helmchen, W. Denk, *Nat. Methods* **2005**, *2*, 932–940.
[7] a) C. Xu, W. Zipfel, J. B. Shear, R. M. Williams, W. W. Webb, *Proc. Natl. Acad. Sci. USA* **1996**, *93*, 10763–10768; b) C. Xu, W. W. Webb, *J. Opt. Soc. Am. B* **1996**, *13*, 481–491.
[8] a) K. Kuba, S. Nakayama, *Neurosci. Res.* **1998**, *32*, 281–294; b) C. D. Wilms, H. Schmidt, J. Eilers, *Cell Calcium* **2006**, *40*, 73–79.
[9] a) C. L. Slayman, V. V. Moussatos, W. W. Webb, *J. Exp. Biol.* **1994**, *196*, 419–438; b) M. J. Petr, R. D. Wurster, *Cell Calcium* **1997**, *21*, 233–240.
[10] a) H. M. Kim, P. R. Yang, M. S. Seo, J.-S. Yi, J. H. Hong, S.-J. Jeon, Y.-G. Ko, K. J. Lee, B. R. Cho, *J. Org. Chem.* **2007**, *72*, 2088–2096; b) H. M. Kim, C. Jung, B. R. Kim, S.-Y. Jung, J. H. Hong, Y.-G. Ko, K. J. Lee, B. R. Cho, *Angew. Chem.* **2007**, *119*, 3550–3553; *Angew. Chem. Int. Ed.* **2007**, *46*, 3460–3463.
[11] a) R. Y. Tsien, *Biochemistry* **1980**, *19*, 2396–2404; b) R. Y. Tsien, *Nature* **1981**, *290*, 527–528.
[12] K. A. Connors, *Binding Constants*, Wiley, New York, **1987**.
[13] J. R. Long, R. S. Drago, *J. Chem. Educ.* **1982**, *59*, 1037–1039.
[14] H. R. Parri, T. M. Gould, V. Crunelli, *Nat. Neurosci.* **2001**, *4*, 803–812.
[15] J. Y. Koh, S. W. Suh, B. J. Gwag, Y. Y. He, C. Y. Hsu, D. W. Choi, *Science* **1996**, *272*, 1013–1016.
[16] C. M. Matias, N. C. Matos, M. Arif, J. C. Dionisio, M. E. Quinta-Ferreira, *Biol. Res.* **2006**, *39*, 521–530.

